Extended fully-nonlinear and strongly-dispersive internal wave equations in a three-layer system

Keisuke Nakayama
Kobe University
nakayama@phoenix.kobe-u.ac.jp

Kenji Shimizu
Formerly at CSIRO Oceans and Atmosphere
kenji.shimizu.rc@gmail.com

Abstract

The KdV, MKdV, Boussinesq-type, Benjamin-Ono, NLS, and eKdV equations have been applied to analyze nonlinear internal waves in a two-layer system. The KP and Boussinesq-type equations have also been used for the analysis of two-layer motions with two horizontal dimensions. However, there are only few equations for a three-layer system applicable to particular or special conditions, such as breather solutions in a three-layer system based on the Gardner equation. Nakayama et al. (2015) have proposed the Fully-nonlinear and strongly-Dispersive Internal wave equations in a three-Layer System (FDI-3LS equations) by extending the two dimensional counterpart (FDI-2LS equations; Nakayama and Kakinuma, 2010), which successfully reproduced a large-amplitude Mach stem due to soliton resonance. This study aims to investigate the applicability of the FDI-3LS equations to analyze internal waves in a three-layer system.

1 Introduction

Monismith (1986) demonstrated that Wedderburn Number (Thompson and Imberger, 1980) could be useful for evaluating upwelling phenomena in a three-layer stratification with constant density in the upper and bottom layers and a linear transition between the two. Imberger and Patterson (1990) revealed that the occurrence of upwelling in the

laboratory experiments by Monismith (1986) can be modeled by introducing Lake Number. Stevens and Imberger (1996) also found that upwelling phenomena can be categorized by using Wedderburn Number and Lake Number. On the other hand, Al-Zanaidi and Dore (1976) revealed a reverse intrusion inside of the density transition layer when internal waves propagate in a two-layer system. Al-Zanaidi and Dore (1976) also found that, unlike the intrusion shown in Nakayama and Imberger (2010) and Nakayama et al. (2012), the reverse intrusion occurs irrespective of the occurrence of internal wave breaking due to topographical effects. The same phenomena were also found in the field observations by Inall et al. (2001) and in the laboratory experiments by Nguyen (2013) in a three-layer system with a density interface between the top and bottom layers.

There have been many equations for the analysis of a one-layer or two-layer system. For example, the KdV, MKdV, Boussinesq-type, Benjamin-Ono, NLS, eKdV and KP equations have been applied to analyze nonlinear internal waves. However, there are only few studies regarding the analysis of a three-layer system using fully-nonlinear and strongly-dispersive effects. As one of the fully-nonlinear and strongly-dispersive wave equations, Nakayama and Kakinuma (2010) proposed the FDI-2LS equations. The FDI-2LS equations can satisfy the dispersion relation in a two-layer system by introducing velocity potential expressed as power function of the z-coordinate (Nakayama and Kakinuma, 2010). Also, the FDI-2LS equations have been revealed to reproduce internal solitary waves more accurately than the Boussinesq-type equations by taking into account the quadratic or cubic term in the velocity potential. Therefore, this study aims to extend the FDI-2LS equations to a three-layer system and to investigate the applicability of the proposed equations in a three-layer system.

2 Fully-nonlinear and strongly-Dispersive Internal wave equations

Three layers of an inviscid and incompressible fluid are considered as shown in **Figure 1,** where three layers are indicated as $i = 1$, $i = 2$ and $i = 3$ from the top to bottom. The depth and density of each layer is indicated by h_i and ρ_i, respectively, with $\rho_1 < \rho_2 < \rho_3$. By assuming irrotational flow, velocity potential ϕ_i is introduced as:

$$\mathbf{u}_i = \nabla\phi_i \quad \text{and} \quad w_i = \frac{\partial \phi_i}{\partial z} \tag{1}$$

$$\nabla = \left(\frac{\partial}{\partial x}, \frac{\partial}{\partial y} \right) \tag{2}$$

where $\mathbf{u}_i$ is the horizontal velocity vector for the layer i, and w_i is the vertical velocity for the layer i.

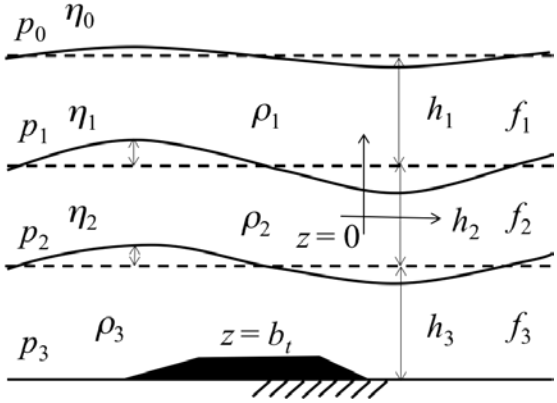

Figure 1 Three-layer system for FDI-3LS equations

The functional for the variational problem is obtained as (3) by adding terms for interfacial pressure into the variational method by Luke (1967).

$$F_i\left[\phi_i, \eta_{i,j}\right] = \int_{t_0}^{t_1} \iint_A \int_{\eta_{i,0}}^{\eta_{i,1}} \left\{ \frac{\partial \phi_i}{\partial t} + \frac{1}{2}\left(\nabla\phi_i\right)^2 + \frac{1}{2}\left(\frac{\partial \phi_i}{\partial z}\right)^2 + gz + \frac{p_{i-j} + P_i}{\rho_i} \right\} dz\, dA\, dt \tag{3}$$

where ϕ_i is the velocity potential of the i^{th} layer, g is the gravitational acceleration, ρ_i is the density of i^{th} layer, p_i is the pressure at the bottom of the i^{th} layer, and P_i is the static pressure of the i^{th} layer. P_i depends on the vertical coordinate system. The velocity potential is defined by equation (4) as a function of the vertical coordinates.

$$\phi_i\left(x,z,t\right) = \sum_{\alpha=0}^{N-1} Z_{i,\alpha}\left\{z, h_i\left(x\right)\right\} f_{i,\alpha}\left(x,t\right) \tag{4}$$

where $Z_{i,}$ is the vertical profile function of α in the i^{th} layer, $\phi_{i,}$ is the weight for α in the i^{th} layer, respectively. j is 0 or 1 that corresponds to the lower or upper boundary of the i^{th} layer. By defining $Z_{i,}$ in (4) as power function of the vertical coordinate system as (5), the Fully-nonlinear and strongly-Dispersive Internal wave equations in a three-layer

System (FDI-3LS) are given from (6) to (17).

$$Z_{i,\alpha} = z^{\alpha} \tag{5}$$

$$\eta_0^a \frac{\partial \eta_0}{\partial t} - \eta_1^a \frac{\partial \eta_1}{\partial t} + \mathrm{R}_{\alpha\beta} \nabla \left\{ \left(\eta_0^{\alpha+\beta+1} - \eta_1^{\alpha+\beta+1} \right) \nabla f_{1,\beta} \right\} - \mathrm{S}_{\alpha\beta} \left(\eta_0^{\alpha+\beta+1} - \eta_1^{\alpha+\beta+1} \right) f_{1,\beta} = 0 \tag{6}$$

$$\eta_0^{\beta} \frac{\partial f_{1,\beta}}{\partial t} + \frac{1}{2} \eta_0^{\beta+\gamma} \nabla f_{1,\beta} \nabla f_{1,\gamma} + \frac{\beta\gamma}{2} \eta_0^{\beta+\gamma-2} f_{1,\beta} f_{1,\gamma} + g\eta_0 + \frac{p_0 + P_1}{\rho_1} = 0 \tag{7}$$

$$\eta_1^{\beta} \frac{\partial f_{1,\beta}}{\partial t} + \frac{1}{2} \eta_1^{\beta+\gamma} \nabla f_{1,\beta} \nabla f_{1,\gamma} + \frac{\beta\gamma}{2} \eta_1^{\beta+\gamma-2} f_{1,\beta} f_{1,\gamma} + g\eta_1 + \frac{p_1 + P_1}{\rho_1} = 0 \tag{8}$$

$$\eta_1^a \frac{\partial \eta_1}{\partial t} - \eta_2^a \frac{\partial \eta_2}{\partial t} + \mathrm{R}_{\alpha\beta} \nabla \left\{ \left(\eta_1^{\alpha+\beta+1} - \eta_2^{\alpha+\beta+1} \right) \nabla f_{2,\beta} \right\} - \mathrm{S}_{\alpha\beta} \left(\eta_1^{\alpha+\beta-1} - \eta_2^{\alpha+\beta-1} \right) f_{2,\beta} = 0 \tag{9}$$

$$\eta_1^{\beta} \frac{\partial f_{2,\beta}}{\partial t} + \frac{1}{2} \eta_1^{\beta+\gamma} \nabla f_{2,\beta} \nabla f_{2,\gamma} + \frac{\beta\gamma}{2} \eta_1^{\beta+\gamma-2} f_{2,\beta} f_{2,\gamma} + g\eta_1 + \frac{p_1 + P_2}{\rho_2} = 0 \tag{10}$$

$$\eta_2^{\beta} \frac{\partial f_{2,\beta}}{\partial t} + \frac{1}{2} \eta_2^{\beta+\gamma} \nabla f_{2,\beta} \nabla f_{2,\gamma} + \frac{\beta\gamma}{2} \eta_2^{\beta+\gamma-2} f_{2,\beta} f_{2,\gamma} + g\eta_2 + \frac{p_2 + P_2}{\rho_2} = 0 \tag{11}$$

$$\eta_2^a \frac{\partial \eta_1}{\partial t} - \mathrm{b}_T^a \frac{\partial \mathrm{b}}{\partial t} + \mathrm{R}_{\alpha\beta} \nabla \left\{ \left(\eta_1^{\alpha+\beta+1} - \mathrm{b}_T^{\alpha+\beta+1} \right) \nabla f_{2,\beta} \right\} - \mathrm{S}_{\alpha\beta} \left(\eta_1^{\alpha+\beta-1} - \mathrm{b}_T^{\alpha+\beta-1} \right) f_{3,\beta} = 0 \tag{12}$$

$$\eta_2^{\beta} \frac{\partial f_{3,\beta}}{\partial t} + \frac{1}{2} \eta_2^{\beta+\gamma} \nabla f_{3,\beta} \nabla f_{3,\gamma} + \frac{\beta\gamma}{2} \eta_2^{\beta+\gamma-2} f_{3,\beta} f_{3,\gamma} + g\eta_2 + \frac{p_2 + P_3}{\rho_3} = 0 \tag{13}$$

$$b_T^{\beta} \frac{\partial f_{3,\beta}}{\partial t} + \frac{1}{2} b_T^{\beta+\gamma} \nabla f_{3,\beta} \nabla f_{3,\gamma} + \frac{\beta\gamma}{2} b_T^{\beta+\gamma-2} f_{3,\beta} f_{3,\gamma} + g b_T + \frac{p_3 + P_3}{\rho_3} = 0 \tag{14}$$

$$P_1 = 0 \tag{15}$$

$$P_2 = -\left(\rho_2 - \rho_1 \right) g \frac{h_2}{2} \tag{16}$$

$$P_3 = \left(\rho_3 - \rho_1 \right) g \frac{h_2}{2} \tag{17}$$

where, b_T is the bottom level, summation convention applies to α and β, and $\mathrm{R}_{\alpha\beta}$ and $\mathrm{S}_{\alpha\beta}$ are coefficients. The same numerical scheme as Nakayama and Kakinuma (2010) was applied. Please see Nakayama and Kakinuma (2010) for more details.

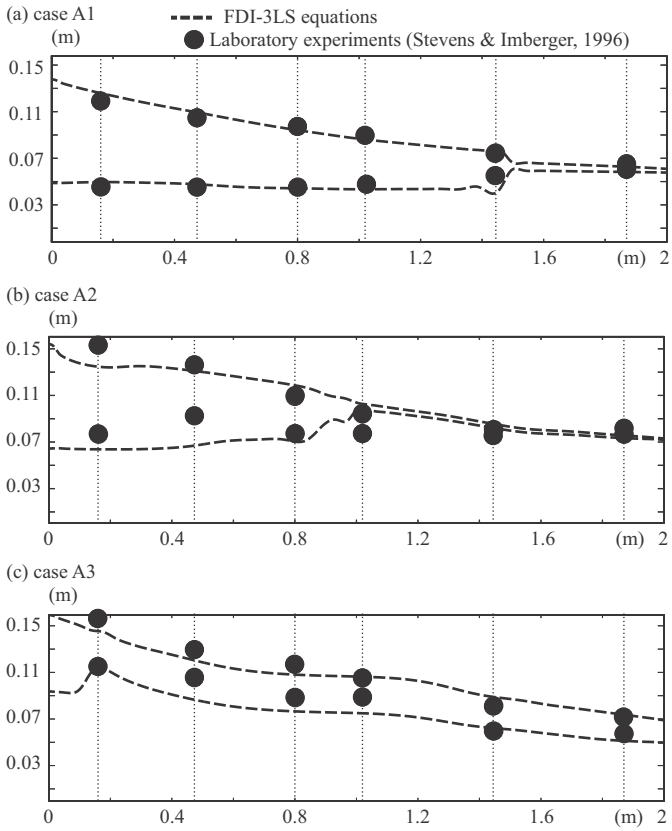

Figure 2 Comparisons between Stevens and Imberger (1996) and FDI-3LS.

3 Result and Conclusion

We applied the FDI-3LS equations to the three-layer laboratory experiments in a tank with the length of 2 m and the water depth of 0.16 m, in which wind stress was given by a belt-type shear maker in order to investigate upwelling phenomena (Stevens and Imberger, 1996) (Figure 2). The Wedderburn Number (WN) was 0.9 and the Lake Number (LN) was 2.0 in Case A1, which showed that the upper density interface reached the water surface and the displacement of the lower density interface was small (WN<1 and LN>1) (black circles in Figure 2). Case A2 is similar to Case A1, but wind stress was larger than case A1 (WN=0.5 and LN=1.1). In case A3, the upper density interface was found to reach the water surface very rapidly compared to the other two cases due to the smaller WN and LN (WN=0.07 and LN=0.35). The FDI-3LS equations successfully reproduced the density interface motions for all the cases (broken lines in Figure 2). It was found from the numerical simulations that non-hydrostatic effect was

significant for the second mode internal waves in the experiments.

References

Al-Zanaidi, M.A. and Dore, B.D. (1976) Some aspects of internal wave motions, *Pageoph*, 114:403-414.

Imberger, J. & Patterson, J.C. (1990). Physical Limnology, *Adv. Appl. Mech.*, 27:303-475.

Inall, M. E., Shapiro, G. I. & Sherwin, T. J. (2001). Mass transport by non-linear internal waves on the Malin Shelf, *J. Cont. Shelf. Res.*, 21:1449-1472.

Luke, J.C. (1967). A variational principle for a fluid with a free surface, *J. Fluid Mech.*, 27:395-397.

Monismith, S. (1986). An experimental study of the upwelling response of stratified reservoirs to surface shear stress, *J. Fluid Mech.*, 171:407-439.

Nakayama, K. & Imberger, J. (2010). Residual circulation due to internal waves shoaling on a slope, *Limnol. Oceanogr.*, 55:1009-1023.

Nakayama, K. & Kakinuma, T. (2010). Internal waves in a two-layer system using fully nonlinear internal-wave equations, *Int. J. Numer. Methods Fluids*, 62(5):574-590.

Nakayama, K., Shintani, T., Kokubo, K., Maruya, Y., Kakinuma, T., Komai, K. & Okada, T., Residual current over a uniform slope due to breaking of internal waves in a two-layer system, *J. Geophys. Res.*, 117:C10002.

Nakayama, K., Yoshie, Y., Shintani, T., Kakinuma, T., Nguyen, H.D., Sato, Y. & Katsuaki, K. (2015). Analysis of wind-induced response of a stratified lake by fully-nonlinear and strongly-dispersive three-layer model. *Ann. J. Hydraulic Eng.*, 71(4):793-798.

Nguyen, K.C. (2013). Visualization and numerical analyses for mass transport due to internal waves propagating in the density-stratified water with a diffusive transition layer, *Doctor thesis of Tokyo Metropolitan University*, 1-117.

Stevens, C. & Imberger, J. (1996). The initial response of a stratified lake to a surface shear stress, *J. Fluid Mech.*, 312:39-66.

Thompson, R.O.R.Y. & Imberger, J. (1980). Response of a numerical model of a stratified lake to wind stress. *Proceedings of Int. Symp.* on Stratified Flows, 562-570.